Neuroscience Informatics 2 (2022) 100093

Contents lists available at ScienceDirect

Neuroscience Informatics

www.elsevier.com/locate/neuri

Original article

Hemodynamic response function (HRF) as a novel brain marker: Applications in subjective cognitive decline (SCD)

Liang Lu, Guangfei Li, Zeyu Song, Zhao Zhang, Xiaoying Tang *

Department of Biomedical Engineering, Beijing Institute of Technology, Beijing, China

ARTICLE INFO

Article history:
Received 29 April 2022
Received in revised form 19 June 2022
Accepted 23 June 2022

Keywords:
Subjective cognitive decline (SCD)
Alzheimer's disease (AD)
Hemodynamic response function (HRF)
Functional magnetic resonance imaging (fMRI)

ABSTRACT

Objective: Subjective cognitive decline (SCD) is the first clinical manifestation of the Alzheimer's disease (AD) continuum. Hemodynamic response function (HRF) carries information related to brain pathology and function. The shape of the HRF can be described by three parameters: response height (RH), time-to-peak (TTP), and full-width at half-max (FWHM). We proposed and explored our two hypotheses. Hypothesis 1: HRF was pathologically related to SCD: compared with healthy controls (HC), patients with SCD show HRF aberrations. Hypothesis 2: HRF could be employed as a novel marker of brain imaging for the classification of SCD.

Methods: We used resting-state functional magnetic resonance imaging (fMRI) data and performed deconvolution to investigate the HRF parameters in 54 individuals with SCD and 64 HC. Statistical two-sample t tests were performed to investigate between-group differences in HRF parameters. Finally, we used logistic regression to construct a binary classification of SCD and HC.

Results: We found altered HRF parameters in the SCD group compared to HC. In the brain regions with altered HRF, we found that RH and FWHM decreased in the SCD group compared to HC, while TTP increased in the SCD group. From the binary logistic regression, we found that the classification accuracy of SCD and HC was 94.07%.

Conclusion: The study demonstrated altered HRF parameters in patients with SCD, which could be used as a novel marker of brain function for the classification of SCD.

1. Introduction

Subjective cognitive decline (SCD) refers to patients' subjective decline in sensory memory and cognitive function compared with the previous normal state, in the case of normal neuropsychological function. The term SCD was conceived by scientists in 2014 [1] and has attracted increasing attention. There is growing evidence that patients with SCD are at increased risk for future pathologic cognitive decline, mild cognitive impairment and Alzheimer's disease (AD) [1]. In addition to subjective cognitive decline without neuropsychological deficits, SCD can affect social functioning, mood and quality of life [2]. Increasing evidence has suggested that elderly patients with SCD are more likely to exhibit abnormalities in biomarkers consistent with AD pathology [1].

As the population ages, worry about cognitive decline rises during medical visits. Neuropsychological and clinical tests show that concern about cognitive decline may be related to different objective factors of cognitive disorder [3]. Dementia is the most serious form of cognitive impairment, which impairs individuals' daily functioning and causes the ability loss of independence [4,5]. AD is one of the most common pathogenic factors of dementia, and the incidence has risen rapidly in recent years. According to the World Alzheimer Report 2018, the number of patients with AD was predicted to reach 115 million by 2050.

Existing treatments are moderately effective in the symptomatic period of AD [6]. At the early stage of AD, patients still have sufficient cognitive functions that can be directly used for functional recovery or compensation [7]. It is important that ongoing biomarker studies are able to diagnose patients with preclinical AD [8], which offers excellent opportunities for treatment success and prevents cognitive decline before the onset of clinical symptoms. As the first clinical manifestation of the AD continuum, SCD is self-perceived cognitive decline without actual cognitive damage [3,7]. SCD is assumed to occur at a comparatively late period of preclinical AD and is closely related to future cognitive decline and dementia [9,10]. Patients with SCD may have biomarker abnormalities consistent with those of AD [1]. However, the association of neuroimaging biomarkers between AD and SCD remains to be fur-

* Corresponding author. Address: Beijing Institute of Technology, 5 South Zhongguancun Street, Beijing 100081, China.
E-mail address: xiaoying@bit.edu.cn (X. Tang).

https://doi.org/10.1016/j.neuri.2022.100093

ther studied [8]. Therefore, studying patients with SCD is of great importance for comprehending preclinical AD pathology and discovering correlated imaging markers, which are essential for the early diagnosis of AD.

With the advent of magnetic resonance imaging (MRI), structural and functional alterations in the brain have been detected during the period of preclinical AD [11,12]. Previous studies of brain imaging have reported functional and structural alterations in patients with SCD. For instance, studies have shown that patients with SCD have a higher amplitude of low-frequency fluctuations (ALFF) in some brain regions that are associated with spontaneous brain activity [13,14]. Despite these findings, previous studies provided inadequate facts on the underlying brain changes in patients with SCD and contributed little to the diagnosis of SCD. In our study, we employed resting-state functional magnetic resonance imaging (fMRI) to find a new neuroimaging biomarker that could be used as an adjunct diagnosis of SCD.

FMRI is a noninvasive technique for detecting neural correlates of brain functioning that monitors brain activity by the blood oxygen level-dependent (BOLD) signal [15]. The neurovascular coupled transfer function model between the BOLD fMRI signal and matching local neural activity is called the hemodynamic response function (HRF) [16]. Studies have shown that the HRF shape could be affected by many factors including nonneural and neural factors [17]. Thus, the shape of HRF has been proven to be different in different individuals and brain regions [18,19]. There are difficulties in interpreting the influence of neural and nonneural factors on HRF shape [18,20]. Given this difficulty, resting-state fMRI studies have generally ignored the variability of HRF because it is so alike in most people that intra-individual variability could be ignored. However, HRF variability has been verified in the brain [18,20]. In addition, previous studies have demonstrated that ignoring HRF could lead to confusion in connectivity estimates [21–24]. Although HRF variability has traditionally been considered confusing, recent studies have proven that HRF carries information related to brain pathology and function, and that information might be unavailable by using conventional fMRI analysis methods [16]. Authors of previous neuroimaging studies have documented the HRF aberrations of individuals with brain diseases compared to healthy controls (HC). For example, aberrations of HRF have been demonstrated in mild traumatic brain injury (mTBI) [25], posttraumatic stress disorder (PTSD) [23], autism spectrum disorders (ASD) [22] and obsessive-compulsive disorder (OCD) [16].

As mentioned above, changes in HRF may indicate degeneration of neurochemical metabolism in the brain. Now, enough evidence has been provided to assume that HRF contains information related to brain pathology. In our study, we aimed to explore whether HRF was related to SCD pathology as tested in samples of patients with SCD and matched HC. The shape of the HRF can be described by three parameters (Fig. 1): response height (RH), time-to-peak (TTP), and full-width at half-max (FWHM) [18,20]. RH is the amplitude of HRF. TTP is a sign of latency, and FWHM is associated with the length of the BOLD signal [16]. In our study, we investigated the relevance of HRF to SCD pathology and the validity of HRF in SCD classification. Given the above situation, we proposed and explored our two hypotheses. Hypothesis 1: HRF was pathologically related to SCD: compared with HC, patients with SCD would show HRF aberrations. Hypothesis 2: HRF could be employed as a novel marker of brain imaging for the classification of SCD.

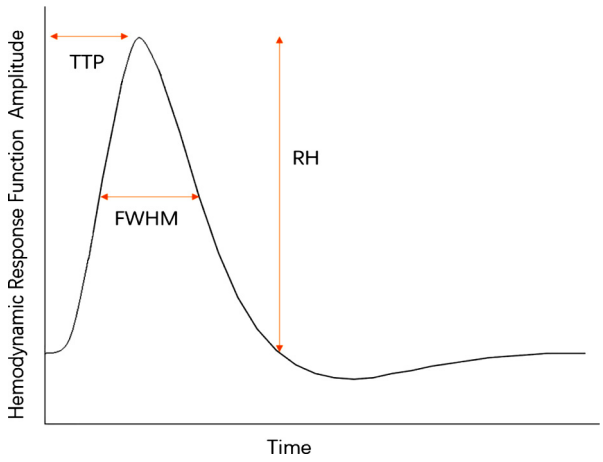

Fig. 1. HRF with its three parameters.

2. Methods

2.1. Participants

124 right-handed subjects (68 HC and 56 SCD) were enrolled from Xuanwu Hospital of Capital Medical University in Beijing, China. The ethics committee of Xuanwu Hospital authorized a standardized clinical protocol. We obtained informed consent from all participants.

Based on the research criteria for SCD [1], the SCD subjects were included according to the following items: (1) self-perceived insistent memory decline compared to state in the past 5 years; (2) normal range scores of standardized neuropsychological tests; (3) score of the Clinical Dementia Rating is zero. The matched HC participants were volunteers with no self-report decline in memory and normal scores of neuropsychological tests. Subjects who met the following criteria were excluded: (1) a history of depression or stroke, or other neurological conditions that may cause cognitive decline (e.g., epilepsy, encephalitis, or Parkinson disease); (2) systemic diseases that may instigate cognitive injuries (e.g., thyroid dysfunctions, HIV or syphilis); (3) traumatic brain injury, congenital mental growth retardation or history of psychosis; and (4) contraindications to MRI or unable to complete neurologic examination.

2.2. FMRI data acquisition and preprocessing

All participants were imaged using a 3 T scanner (GE Healthcare). The resting-state fMRI scan lasted for 8 minutes. The following parameters were used to obtain the T1-weighted MR images: SPGR sequence, repetition time (TR) = 6.9 ms, echo time (TE) = 2.98 ms, inversion time (TI) = 450 ms, flip angle (FA) = 12°, field of view (FOV) = 256×256 mm^2, slice thickness = 1 mm, slice number = 192, matrix = 256×256, no gap and voxel size = 1×1×1 mm^3. Functional images were obtained using the echo plane imaging sequence and the following parameters: TR = 2000 ms, TE = 30 ms, FOV = 224×224 mm^2, FA = 90°, matrix = 64×64, slice number = 28, slice thickness = 4.0 mm, gap = 1.0 mm, and voxel size = 3.5×3.5×4 mm^3. By the way, an experienced neuroradiologist checked all the images for quality and contingency.

The DPABI toolbox [26] was employed to preprocess the fMRI data. The first ten points of each participant of fMRI data were removed to ensure balanced signal saturation. The fMRI data of each participant were realigned and corrected for slice timing. Those functional images were coregistered with matched structural images and then normalized by segmentation. All data were detrended to remove the linear detrending. Low-frequency signals

were removed by a band-pass filter (0.01 Hz–0.1 Hz). A 4 mm Gaussian kernel was employed to smooth all the images. The nuisance covariates were used to regress the global signal including cerebrospinal fluid and white matter signals. Five participants were excluded because relative head motion exceeded 3 mm and one participant was excluded due to data corruption. Finally, the preprocessed data were obtained for forward analysis.

2.3. Deconvolution and HRF estimation

The fMRI data were performed deconvolution to obtain the HRF parameters, employing an emerging technique proposed by Wu et al. [27]. The preprocessed fMRI data were experienced voxel-wise deconvolution over time to extract the underlying neural time series and the HRF parameters of every voxel. Wu et al. [27] have verified the effectiveness of this method by using simulations. Due to its robustness and interpretability, this method has gained more and more acceptance and popularity. Several recent studies have employed this technique (e.g., [16,23,24,28–33]. The results of deconvolution were estimated HRF of every subject at every voxel, which could be described by three parameters: RH, TTP, and FWHM.

2.4. Statistical analysis

We used SPSS 26.0 (SPSS Inc., Chicago, IL, USA) to analyze demographic and clinical variables. We used two-sample t tests to determine differences in age, education level, and Mini–Mental State Examination (MMSE). The χ^2 test was used to compare the gender ratio. $P < 0.05$ was considered statistically significant. Statistical two sample t-tests were performed using Statistical Parametric Mapping (SPM12) (University College London, London, UK) to investigate intergroup differences in HRF. The HRF was characterized by three parameters: RH, TTP, and FWHM, as described. The significance threshold of RH analyses was set at a P value of less than 0.005 and cluster size greater than 70 mm^3. The significance threshold of TTP analyses was set at a P value of less than 0.05 and cluster size greater than 90 mm^3. And the significance threshold of FWHM analyses was set at a P value of less than 0.05 and cluster size greater than 150 mm^3, all of which corresponded to a corrected P value by familywise error (FWE) of less than 0.05.

We defined the brain regions with significant differences as regions of interest (ROI) which were tested by statistical two-sample t tests. Then, We used the REST toolkit [34] to extract signals for ROI. Finally, to verify the validity of the three HRF parameters, we used logistic regression to classify HC and SCD based on SPSS 26.0. The ROI signals of the three HRF parameters were chosen as variables to obtain the classification accuracy. We used the accuracy, sensitivity and specificity as the evaluation indicators of the classifier.

$$\text{Accuracy} = \frac{TP + TN}{TP + FP + TN + FN}$$

$$\text{Sensitivity} = \frac{TP}{TP + FN}$$

$$\text{Specificity} = \frac{TN}{TN + FP}$$

TP, True Positive; TN, True Negative; FP, False Positive; FN, False Negative.

3. Results

3.1. Demographics and clinical variables

The demographic and clinical information of the SCD and HC groups is summarized in Table 1. There were no significant differences ($P > 0.05$ for all) in age, sex, education or MMSE scores between the SCD and HC groups.

Table 1
Demographic and Clinical Characteristics of SCD and HC Groups.

Characteristics	HC (n = 64)	SCD (n = 54)	P value	F value
Age	64.95(5.266)	65.98(5.049)	0.721	0.128
Sex (m/f)	31/33	20/34	0.213	$\lambda^2 = 1.551$
Education	11.88(3.388)	11.83(2.725)	0.353	0.871
MMSE	28.83(1.229)	28.80(1.188)	0.591	0.290

The Chi-square test was used for sex, and two-sample t tests were used for age, education level, MMSE. HC, healthy controls; SCD, subjective cognitive decline; MMSE, Mini-mental State Examination.

Table 2
Regions showing significant RH differences between the SCD and HC groups.

Brain regions	Voxels	MNI Coordinates			$P_{FWE-corr}$
Frontal_Sup_Medial_L	88	−6	30	33	0.007
Frontal_Sup_L	101	−21	39	33	0.003
Frontal_Sup_R	83	24	45	42	0.011
Frontal_Mid_R	75	33	12	54	0.019
Frontal_Inf_Tri_L	72	−54	39	−6	0.024

MNI, Montreal Neurological Institute; $P_{FWE-corr}$, P value corrected by familywise error, Sup, superior; Mid, middle; Inf, inferior; Tri, triangular; L, left; R, right.

Table 3
Regions showing significant TTP differences between the SCD and HC groups.

Brain regions	Voxels	MNI Coordinates			$P_{FWE-corr}$
Cuneus_L	258	3	−90	24	0.000
Precentral_L	227	−36	−24	66	0.000
Frontal_Sup_R	171	15	6	72	0.000
Cerebelum_8_R	97	36	−54	−48	0.018

MNI, Montreal Neurological Institute; $P_{FWE-corr}$, P value corrected by familywise error, Sup, superior; L, left; R, right.

Table 4
Regions showing significant FWHM differences between the SCD and HC groups.

Brain regions	Voxels	MNI Coordinates			$P_{FWE-corr}$
Cuneus_R	3191	3	−81	21	0.000
Fusiform_R	321	36	−69	−18	0.000
Temporal_Pole_Sup_L	340	−33	9	−27	0.000
Rectus_R	188	6	42	−24	0.000
Temporal_Mid_L	530	−63	−48	0	0.000
Frontal_Sup_Medial_R	160	6	60	27	0.002
Caudate_L	247	−3	6	3	0.000

MNI, Montreal Neurological Institute; $P_{FWE-corr}$, P value corrected by familywise error, Sup, superior; Mid, middle; L, left; R, right.

3.2. Abnormal HRF parameters

Aberrations of HRF parameters were found in the SCD group compared to the HC group. Regionally, a lower RH was found in the SCD group than in HC in the left medial superior frontal gyrus ($P = 0.007$), bilateral superior frontal gyrus (left: $P = 0.003$; right: $P = 0.011$), right middle frontal gyrus ($P = 0.019$), and left triangle inferior frontal gyrus ($P = 0.024$) (Table 2, Fig. 2). Slower TTP was detected for the SCD group compared with the HC group in the left cuneus ($P < 0.001$), left precentral gyrus ($P < 0.001$), right superior frontal gyrus ($P < 0.001$), and right cerebellum crus 8 ($P = 0.018$) (Table 3, Fig. 3). Subjects in the SCD group had narrower FWHM values than those in the HC group in the right cuneus ($P < 0.001$), right fusiform gyrus ($P < 0.001$), left temporal pole: superior temporal gyrus ($P < 0.001$), right rectus gyrus ($P < 0.001$), left middle temporal gyrus ($P < 0.001$), right medial superior frontal gyrus ($P = 0.002$), and left caudate nucleus ($P < 0.001$) (Table 4, Fig. 4).

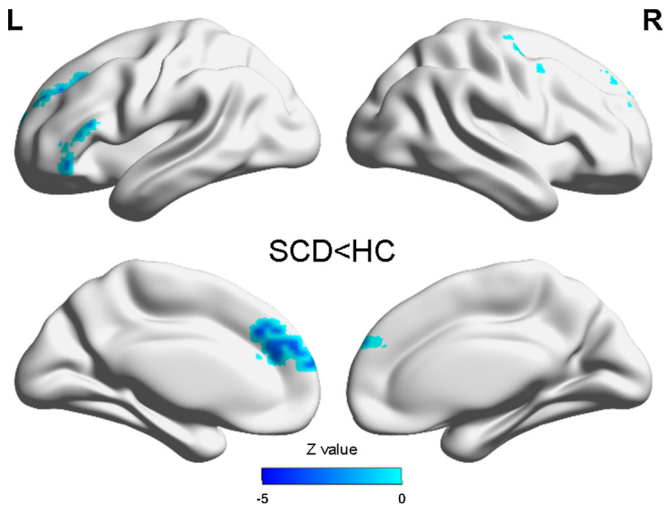

Fig. 2. Lower RH was found in the left medial superior frontal gyrus, bilateral superior frontal gyrus, right middle frontal gyrus, and left triangle inferior frontal gyrus.

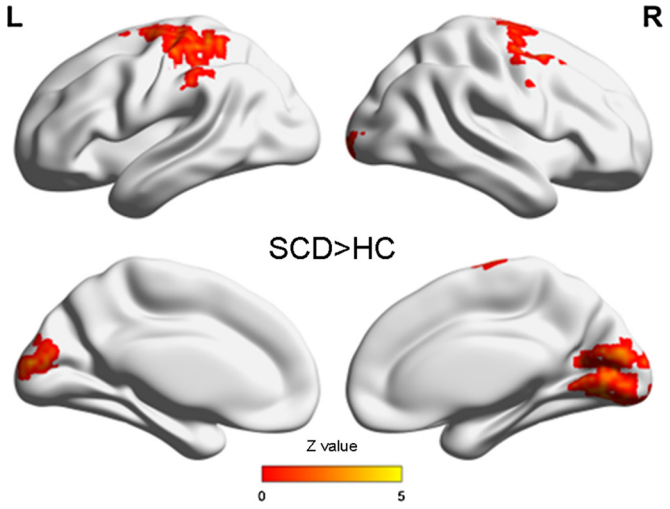

Fig. 3. Slower TTP was found in the left cuneus, left precentral gyrus, right superior frontal gyrus, and right cerebellum crus 8.

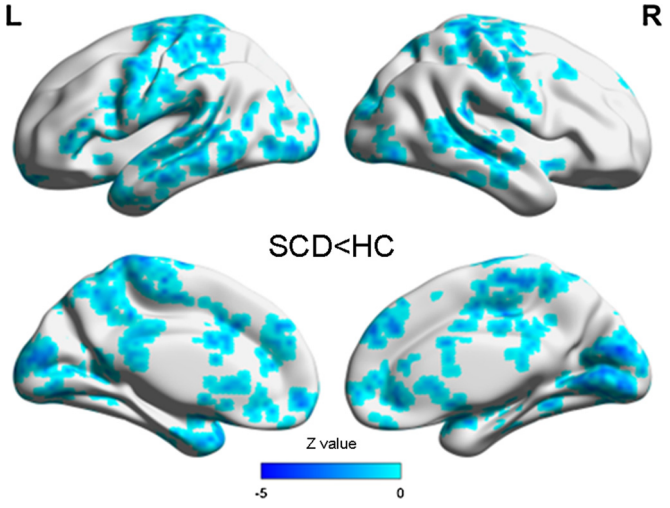

Fig. 4. Narrower FWHM was found in the right cuneus, right fusiform gyrus, left temporal pole: superior temporal gyrus, right rectus gyrus, left middle temporal gyrus, right medial superior frontal gyrus, and left caudate nucleus.

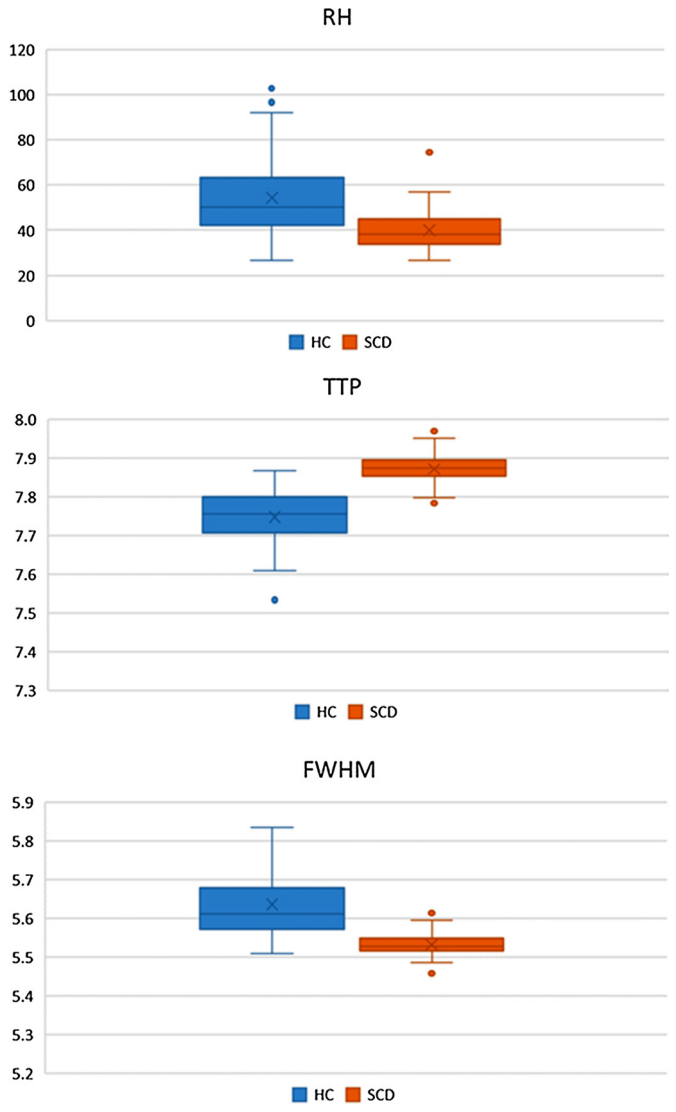

Fig. 5. Boxplots showing lower RH, slower TTP, and narrower FWHM of the ROI regions in the SCD group compared than in the HC group.

Table 5
Results of the Binary Logistical Regression.

Observed	Predicted		Percentage Correct
	HC	SCD	
HC	61	3	95.31
SCD	4	50	92.59

HC, healthy controls; SCD, subjective cognitive decline.

3.3. Binary classification

The three HRF parameters extracted from the defined ROI regions are shown in boxplots (Fig. 5). For the binary logistic regression, the inputs to the classifier were just the three parameters of HRF mentioned earlier, which contributed to verifying our hypotheses. We found that the classification accuracy of SCD and HC was 94.07% (sensitivity = 92.59, specificity = 95.31), which was significantly greater than chance. The classification table is shown in Table 5.

4. Discussion

The aim of our study was to evaluate the correlation between HRF shape and SCD pathology. This aim was driven by previous

research supporting the idea that HRF carries information relevant to brain pathology and function. We hypothesized that HRF was sensitive to SCD pathology and that HRF could be used as a novel marker of brain function for the classification of SCD. In this study, we tested our two hypotheses and found substantial evidence in support of our two hypotheses.

We found altered HRF parameters in the SCD group compared to HC, which could support hypothesis 1 (HRF was pathologically related to SCD). In the brain regions with altered HRF, we found that RH and FWHM decreased in the SCD group compared to HC, while TTP increased in the SCD group. This alteration in HRF has been attributed to metabolic and microvascular disturbances associated with brain disorders [25]. In this study, we found RH differences between SCD patients and HC mainly in the frontal lobe. Alterations in TTP and FWHM were found mainly in the frontal lobe, temporal lobe and occipital lobe. Previous resting-state fMRI studies have revealed abnormal brain activity in these regions with AD risk [35]. Taken together, the results of HRF analysis shared some similarities with findings from previous conventional fMRI analyses, but there were also significant differences, suggesting that HRF might provide novel insights. In this study, we found altered HRF in patients with SCD, suggesting a possible compensatory mechanism in early AD.

We also found strong evidence to support hypothesis 2 (HRF could be used as a novel marker of brain function for the classification of SCD). From the binary logistic regression, we found that the classification accuracy of SCD and HC was 94.07%, much higher than a recent study that combined support vector machine classifier and brain structural network features to discriminate SCD and NC with an accuracy of 83.9% [36]. More importantly, the inputs of our classifier were just the three HRF parameters, proving that HRF could be used as a novel marker for the diagnosis of SCD.

Our study was the first to find that abnormal HRF may aid in the early diagnosis of SCD. We found HRF changes in SCD, which proved our hypotheses. More importantly this study provided new evidence for the HRF parameters extracted from fMRI as a marker of brain function and pathology. HRF parameter estimation is fundamentally different from traditional fMRI measures, which may provide new perspectives and insights unavailable through traditional methods. In addition, a better understanding of HRF parameters from future studies may reveal additional insights.

There were several limitations to this study. First, the small sample size could restrict the statistical power of the results. More participants need to be included in further study. Second, the HRF aberrations observed in this study should be interpreted with caution, since this was the first study with the applications of HRF in SCD pathology. Third, this study was cross-sectional. A longitudinal study would be helpful to explore the association between HRF and SCD severity. In the future, we plan to expand the data sample size and use machine learning methods to further study the classification effect of HRF.

5. Conclusions

The SCD group had altered HRF parameters compared to HC. In the brain regions with altered HRF, RH and FWHM decreased in the SCD group compared to HC, while TTP increased in the SCD group. Furthermore, the study demonstrated that altered HRF parameters could be used as a novel marker of brain function for the classification of SCD. The findings provided evidence for the HRF parameters extracted from fMRI as a marker of brain function and pathology, which could provide new perspectives and methods for SCD and early AD pathology.

Declaration of competing interest

The authors declare that they have no known competing financial or personal relationships that could be viewed as influencing the work reported in this paper.

Funding

This work has been supported by: The National Natural Science Foundation of China (U20A20388).

Author contributions

All authors attest that they meet the current International Committee of Medical Journal Editors (ICMJE) criteria for Authorship.

Acknowledgement

We acknowledge Xuanwu Hospital of Capital Medical University for providing the data in this study.

References

[1] F. Jessen, et al., A conceptual framework for research on subjective cognitive decline in preclinical Alzheimer's disease, (in eng) Alzheimer's Dement. 10 (6) (Nov 2014) 844–852.
[2] A. Jenkins, A. Tales, J. Tree, A. Bayer, Are we ready? The construct of subjective cognitive impairment and its utilization in clinical practice: a preliminary UK-based service evaluation, (in eng) J. Alzheimer's Dis. 48 (Suppl 1) (Sep 24 2015) S25–S31.
[3] F. Jessen, et al., The characterisation of subjective cognitive decline, (in eng), Lancet Neurol. 19 (3) (Mar 2020) 271–278.
[4] G.M. McKhann, et al., The diagnosis of dementia due to Alzheimer's disease: recommendations from the national institute on aging-Alzheimer's association workgroups on diagnostic guidelines for Alzheimer's disease, (in eng), Alzheimer's Dement. 7 (3) (May 2011) 263–269.
[5] B. Winblad, et al., Defeating Alzheimer's disease and other dementias: a priority for European science and society, (in eng), Lancet Neurol. 15 (5) (Apr 2016) 455–532.
[6] S.S. Ong, P.M. Doraiswamy, E.M. Lad, Controversies and future directions of ocular biomarkers in Alzheimer disease, (in eng), JAMA Neurol. 75 (6) (Jun 1 2018) 650–651.
[7] L.A. Rabin, C.M. Smart, R.E. Amariglio, Subjective cognitive decline in preclinical Alzheimer's disease, (in eng), Annu. Rev. Clin. Psychol. 13 (May 8 2017) 369–396.
[8] X. Wang, et al., Neuroimaging advances regarding subjective cognitive decline in preclinical Alzheimer's disease, (in eng), Mol. Neurodegener. 15 (1) (Sep 22 2020) 55.
[9] C.R. Jack Jr., et al., NIA-AA research framework: toward a biological definition of Alzheimer's disease, (in eng), Alzheimer's Dement. 14 (4) (Apr 2018) 535–562.
[10] R.E.R. Slot, et al., Subjective cognitive decline and rates of incident Alzheimer's disease and non-Alzheimer's disease dementia, (in eng), Alzheimer's Dement. 15 (3) (Mar 2019) 465–476.
[11] E. Mak, et al., Structural neuroimaging in preclinical dementia: from microstructural deficits and grey matter atrophy to macroscale connectomic changes, (in eng), Ageing Res. Rev. 35 (May 2017) 250–264.
[12] M. Habib, et al., Functional neuroimaging findings in healthy middle-aged adults at risk of Alzheimer's disease, (in eng) Ageing Res. Rev. 36 (Jul 2017) 88–104.
[13] Y. Sun, et al., Subjective cognitive decline: mapping functional and structural brain changes-a combined resting-state functional and structural MR imaging study, (in eng), Radiology 281 (1) (Oct 2016) 185–192.
[14] L. Yang, et al., Gradual disturbances of the amplitude of low-frequency fluctuations (ALFF) and fractional ALFF in Alzheimer spectrum, (in eng), Front. Neurosci. 12 (2018) 975.
[15] H. Wei, A.M. Frey, A. Jasanoff, Molecular fMRI of neurochemical signaling, (in eng), J. Neurosci. Methods 364 (Dec 1 2021) 109372.
[16] D. Rangaprakash, R. Tadayonnejad, G. Deshpande, J. O'Neill, J.D. Feusner, FMRI hemodynamic response function (HRF) as a novel marker of brain function: applications for understanding obsessive-compulsive disorder pathology and treatment response, (in eng), Brain Imaging Behav. 15 (3) (Jun 2021) 1622–1640.
[17] F. Biessmann, Y. Murayama, N.K. Logothetis, K.R. Müller, F.C. Meinecke, Improved decoding of neural activity from fMRI signals using non-separable spatiotemporal deconvolutions, (in eng), NeuroImage 61 (4) (Jul 16 2012) 1031–1042.

[18] D.A. Handwerker, J.M. Ollinger, M. D'Esposito, Variation of BOLD hemodynamic responses across subjects and brain regions and their effects on statistical analyses, (in eng), NeuroImage 21 (4) (Apr 2004) 1639–1651.
[19] D.A. Handwerker, J. Gonzalez-Castillo, M. D'Esposito, P.A. Bandettini, The continuing challenge of understanding and modeling hemodynamic variation in fMRI, (in eng), NeuroImage 62 (2) (Aug 15 2012) 1017–1023.
[20] G.K. Aguirre, E. Zarahn, M. D'Esposito, The variability of human, BOLD hemodynamic responses, (in eng), NeuroImage 8 (4) (Nov 1998) 360–369.
[21] W. Yan, D. Rangaprakash, G. Deshpande, Estimated hemodynamic response function parameters obtained from resting state BOLD fMRI signals in subjects with autism spectrum disorder and matched healthy subjects, (in eng), Data Brief 19 (Aug 2018) 1305–1309.
[22] W. Yan, D. Rangaprakash, G. Deshpande, Aberrant hemodynamic responses in autism: implications for resting state fMRI functional connectivity studies, (in eng), NeuroImage Clin. 19 (2018) 320–330.
[23] D. Rangaprakash, M.N. Dretsch, W. Yan, J.S. Katz, T.S. Denney Jr., G. Deshpande, Hemodynamic variability in soldiers with trauma: implications for functional MRI connectivity studies, (in eng), NeuroImage Clin. 16 (2017) 409–417.
[24] D. Rangaprakash, G.R. Wu, D. Marinazzo, X. Hu, G. Deshpande, Hemodynamic response function (HRF) variability confounds resting-state fMRI functional connectivity, (in eng), Magn. Reson. Med. 80 (4) (Oct 2018) 1697–1713.
[25] A.R. Mayer, T. Toulouse, S. Klimaj, J.M. Ling, A. Pena, P.S. Bellgowan, Investigating the properties of the hemodynamic response function after mild traumatic brain injury, (in eng), J. Neurotrauma 31 (2) (Jan 15 2014) 189–917.
[26] C.G. Yan, X.D. Wang, X.N. Zuo, Y.F. Zang, DPABI: data processing & analysis for (resting-state) brain imaging, (in eng), Neuroinformatics 14 (3) (Jul 2016) 339–351.
[27] G.R. Wu, W. Liao, S. Stramaglia, J.R. Ding, H. Chen, D. Marinazzo, A blind deconvolution approach to recover effective connectivity brain networks from resting state fMRI data, (in eng), Med. Image Anal. 17 (3) (Apr 2013) 365–374.
[28] D. Rangaprakash, et al., Compromised hippocampus-striatum pathway as a potential imaging biomarker of mild-traumatic brain injury and posttraumatic stress disorder, (in eng), Hum. Brain Mapp. 38 (6) (Jun 2017) 2843–2864.
[29] D. Rangaprakash, M.N. Dretsch, W. Yan, J.S. Katz, T.S. Denney Jr., G. Deshpande, Hemodynamic response function parameters obtained from resting-state functional MRI data in soldiers with trauma, (in eng), Data Brief 14 (Oct 2017) 558–562.
[30] D. Rangaprakash, M.N. Dretsch, A. Venkataraman, J.S. Katz, T.S. Denney Jr., G. Deshpande, Identifying disease foci from static and dynamic effective connectivity networks: illustration in soldiers with trauma, (in eng), Hum. Brain Mapp. 39 (1) (Jan 2018) 264–287.
[31] E. Amico, et al., Posterior cingulate cortex-related co-activation patterns: a resting state FMRI study in propofol-induced loss of consciousness, (in eng), PLoS ONE 9 (6) (2014) e100012.
[32] B. Lamichhane, B.M. Adhikari, S.F. Brosnan, M. Dhamala, The neural basis of perceived unfairness in economic exchanges, (in eng), Brain Connect. 4 (8) (Oct 2014) 619–630.
[33] M. Boly, et al., Stimulus set meaningfulness and neurophysiological differentiation: a functional magnetic resonance imaging study, (in eng), PLoS ONE 10 (5) (2015) e0125337.
[34] X.W. Song, et al., REST: a toolkit for resting-state functional magnetic resonance imaging data processing, (in eng), PLoS ONE 6 (9) (2011) e25031.
[35] I.M. McDonough, S.B. Festini, M.M. Wood, Risk for Alzheimer's disease: a review of long-term episodic memory encoding and retrieval fMRI studies, (in eng), Ageing Res. Rev. 62 (Sep 2020) 101133.
[36] W. Huang, X. Li, X. Li, G. Kang, Y. Han, N. Shu, Combined support vector machine classifier and brain structural network features for the individual classification of amnestic mild cognitive impairment and subjective cognitive decline patients, (in eng), Front. Aging Neurosci. 13 (2021) 687927.